CENTRAL ASIAN JOURNAL OF THEORETICAL AND APPLIED SCIENCE

https://cajotas.casjournal.org/index.php/cajotas

Volume: 07 Issue: 03 | July 2026 ISSN: 2660-5317

Article

Long-Term MgSO4 Durability of CFRP-Strengthened NSC and UHPC Beams: Surface Preparation Effects on Bond-Dependent Flexural Performance

Shahad Majid Madhlom[1], Prof. Dr. Hussam Ali Mohammed[2]

1. Al-Furat Al-Awsat Technical University, Al-Mussaib Technical College, Department of Building and Construction Engineering

* Correspondence: shahad.majid.tcm36@student.atu.edu.iq, com.hus@atu.edu.iq

Abstract: The long-term effectiveness of externally bonded carbon fiber-reinforced polymer (CFRP) strengthening systems is strongly governed by the durability and stress-transfer capacity of the CFRP–epoxy–concrete interface. This study experimentally investigates the bond-dependent flexural performance of CFRP-strengthened normal-strength concrete (NSC) and ultra-high-performance concrete (UHPC) beams after exposure to magnesium sulfate solution. Twelve reinforced concrete beams were tested, including six NSC beams and six UHPC beams. For each concrete type, one unstrengthened control beam was used as a reference, while the remaining beams were strengthened with a single externally bonded CFRP sheet after applying mechanical grinding, vertical grooving, 45° inclined grooving, sandblasting, or diluted HCl treatment. After CFRP bonding and seven days of epoxy curing, all specimens were immersed in a 3.5% $MgSO_4$ solution for 120 days before flexural testing under two-point loading.

The results showed that CFRP strengthening remained effective after sulfate conditioning, although the improvement depended strongly on surface preparation and substrate type. In the NSC group, sandblasting produced the highest ultimate load of 145.70 kN, corresponding to a 20.55% increase over the control beam. In the UHPC group, sandblasting also achieved the highest ultimate load of 205.20 kN, representing a 28.12% increase. The 45° inclined grooving technique achieved a comparable ultimate load of 202.89 kN and provided the highest UHPC stiffness response, with a secant stiffness of 40.96 kN/mm and a 47.28% increase over the control specimen. Overall, sandblasting was most effective for load enhancement, whereas 45° inclined grooving provided a more balanced long-term response in terms of strength, stiffness, deformation behavior, and interface stability.

Keywords: Carbon fiber-reinforced polymer; Ultra-high-performance concrete; Magnesium sulfate exposure; Surface preparation; CFRP–epoxy–concrete interface; Long-term durability; Flexural behavior.

Citation: Madhlom, S. M & Mohammed, H. A. Long-Term MgSO4 Durability of CFRP-Strengthened NSC and UHPC Beams: Surface Preparation Effects on Bond-Dependent Flexural Performance. Central Asian Journal of Theoretical and Applied Science 2026, 7(3), 185-203

Received: 10th Mar 2026
Revised: 21th Apr 2026
Accepted: 08th May 2026
Published: 02th June 2026

1. Introduction

Background and engineering problem

Externally bonded carbon fiber-reinforced polymer (CFRP) systems have been widely used for the strengthening and rehabilitation of reinforced concrete structures because of their high strength-to-weight ratio, corrosion resistance, and ease of field application [1]. In flexural strengthening applications, CFRP laminates bonded to the tension face of reinforced concrete beams can enhance load-carrying capacity and stiffness without significantly increasing the self-weight of the member. However, the effectiveness of this strengthening system is governed not only by the tensile capacity of the CFRP laminate, but also by the ability of the CFRP–epoxy–concrete interface to transfer stresses reliably

after cracking. Premature debonding, plate-end separation, or concrete cover separation may prevent full utilization of the CFRP tensile capacity and lead to brittle failure before the expected design resistance is reached [2].

Ultra-high-performance concrete (UHPC) introduces a more complex bond condition compared with normal-strength concrete (NSC). Its dense microstructure, refined pore system, high compressive strength, and improved tensile response provide excellent mechanical and durability performance. Nevertheless, these same characteristics may restrict epoxy penetration into the near-surface zone, especially when the surface is smooth or insufficiently roughened. Therefore, when CFRP is bonded to UHPC, the surface preparation process becomes a governing factor rather than a secondary construction detail. Mechanical roughening, grooving, sandblasting, and chemical etching can alter the surface texture, increase the effective bonded area, improve mechanical interlock, and modify the stress-transfer mechanism along the CFRP–epoxy–concrete interface [3].

Alkaysi et al. [4] reported that steel-fiber-reinforced UHPC can exhibit post-cracking strain-hardening, characterized by stable multiple cracking, reduced crack widths, and enhanced energy dissipation compared with normal-strength concrete (as shown in Figure 2-3). This tensile/fracture response is directly relevant to CFRP strengthening because crack spacing and crack width govern interfacial shear and peel stress redistribution along the CFRP–epoxy–concrete system, thereby influencing the likelihood of premature debonding, particularly plate-end debonding.

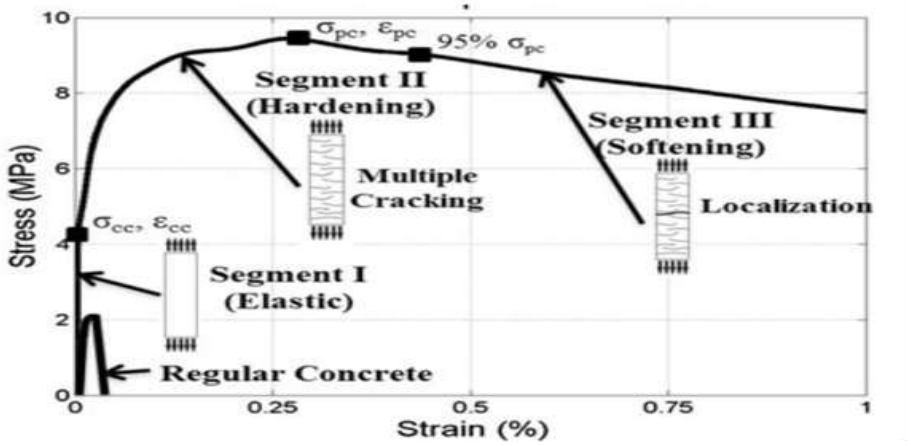

Fig.1: Typical tensile stress - strain response in UHPC [5]

Surface preparation has been widely investigated as a means of improving the CFRP–concrete interface through chemical, mechanical, and groove-based conditioning of the concrete substrate. Yin and Fan demonstrated that roughness level significantly controls CFRP–concrete interfacial response by influencing effective bond length, bond–slip characteristics, and failure mode transition [6]. Similarly, Al-Rousan and AL-Tahat; Soares et al. investigated the influence of different surface preparation techniques on the bond behavior between CFRP sheets and concrete [7][8]. The experimental program included 108 concrete prism specimens tested under double-shear loading.

Li et al. [9] reviewed the durability performance of ultra-high-performance concrete (UHPC) and reported that its dense microstructure, refined pore system, low permeability, and optimized binder matrix provide superior resistance against several deterioration mechanisms, including water and chloride ingress, carbonation, freeze–thaw action, chemical attack, alkali–silica reaction, abrasion, and fire exposure. These durability characteristics make UHPC highly suitable for aggressive infrastructure environments. However, in externally bonded CFRP-strengthened UHPC members, the high durability of the UHPC matrix does not necessarily ensure the long-term durability of the CFRP–epoxy–UHPC interface. The low permeability and compact near-surface structure of UHPC may limit through-thickness penetration, but moisture or sulfate-bearing solutions may still migrate preferentially along the adhesive–substrate interphase. Therefore, the findings of Li et al. [10] support the need to distinguish between

matrix-level UHPC durability and interface-level bond durability, which justifies the evaluation of CFRP–UHPC bond performance after long-term $MgSO_4$ exposure in the present study.

Hazen Masrafata [11] investigated the influence of exposure to a 5% magnesium sulfate ($MgSO_4$) solution on the mechanical properties of Portland composite cement concrete (PCC). The specimens were first cured in water for 28 days and then exposed to $MgSO_4$ solution, with observations conducted before exposure and after 28, 56, and 90 days of immersion. The results showed an initial improvement in compressive strength, reaching an increase of 8.78% after 56 days, followed by a reduction of 7.2% at 90 days compared with the 56-day value. The study also reported that modulus of elasticity, Poisson's ratio, tensile strength, and fracture energy followed the same trend as compressive strength, while the concrete mass increased after 56 days and then decreased at 90 days. These findings indicate that magnesium sulfate exposure may initially produce limited densification or strength gain, but prolonged exposure can initiate sulfate-related deterioration through microcrack development and progressive degradation of mechanical properties. Although this study was conducted on PCC rather than UHPC or CFRP-strengthened concrete, it is relevant to the present work because it demonstrates the time-dependent effect of $MgSO_4$ exposure on cementitious materials and supports the need to evaluate long-term bond durability under sulfate conditioning.

Zhao et al. [12] investigated the effect of magnesium on sulfate-induced deterioration in cast-in-situ concrete by exposing specimens to full and partial immersion in sodium sulfate and magnesium sulfate solutions for 12 months. The results showed that higher sulfate concentration accelerated concrete degradation, while partially immersed specimens suffered more severe damage due to the combined effects of chemical attack and salt crystallization. The study also found that magnesium delayed early strength development, but in later stages it slowed sulfate diffusion and reduced cracking and surface spalling near the immersion level.

Al Mahmoud examined environmental exposure effects on different CFRP strengthening systems and showed that salt-water immersion (3.5% salted water) for 120 days can reduce the ultimate bond capacity of specimens strengthened using externally bonded CFRP sheets, indicating that sustained moisture and chlorides may be detrimental to bond-critical EBR systems and may promote earlier debonding when the interface governs the response. From a materials standpoint [13]. Uthaman et al. reported that epoxy resins and CFRP composites may undergo durability-related property changes under water and chemically aggressive immersion environments [14]. These findings support the expectation that environmental conditioning can weaken the adhesive and/or the near-interface region (e.g., via water uptake and polymer plasticization) and reduce interfacial fracture resistance over time. In parallel, Zhang et al. **c**ompared epoxy-bonded CFRP sheets with cement-bonded CFRP grids under water immersion up to six months and observed a progressive decline in interfacial fracture energy with immersion duration, while failure remained governed by interface/near-interface mechanisms in a system-dependent manner [15]. Cruz et al. further highlighted that moisture-driven ageing can significantly degrade structural epoxy adhesive properties, whereas CFRP laminates are often comparatively less sensitive, implying that durability-induced loss of bond performance in externally bonded systems is frequently controlled by deterioration of the adhesive/interphase rather than by the fiber itself. Collectively, these studies suggest that durability assessment should consider (i) exposure severity and mode (continuous immersion versus wet–dry cycling, temperature, and solution chemistry), (ii) capacity retention alongside fracture-energy/bond–slip indicators, and (iii) potential shifts in the governing failure mechanism with conditioning time.

Although several studies have investigated CFRP strengthening of reinforced concrete beams, the long-term performance of the CFRP–epoxy–UHPC bonded interface under magnesium sulfate exposure remains insufficiently understood. In particular, limited experimental evidence is available on how practical surface preparation techniques affect bond-dependent flexural behavior, debonding resistance, stiffness,

ductility, and failure mode of CFRP-strengthened UHPC beams after prolonged $MgSO_4$ conditioning.

2. Materials and Method

Materials

Two concrete substrates were used in this study: normal-strength concrete (NSC) and ultra-high-performance concrete (UHPC). The NSC mixture was designed to represent a conventional C30 concrete substrate, while the UHPC mixture was designed to represent a high-density and high-strength substrate for evaluating the long-term bond-dependent performance of externally bonded CFRP strengthening. The adopted NSC achieved an average 28-day cylinder compressive strength of 29.3 MPa, a flexural strength of 4.45 MPa, and a splitting tensile strength of 3.30 MPa. In comparison, the adopted UHPC achieved an average 28-day compressive strength of 150.86 MPa, direct tensile strength of 15.40 MPa, splitting tensile strength of 15.67 MPa, and flexural strength of 23.44 MPa. The UHPC mixture incorporated straight copper-coated micro-steel fibers at a dosage of 2% by volume to improve tensile resistance, crack control, and post-cracking behavior.

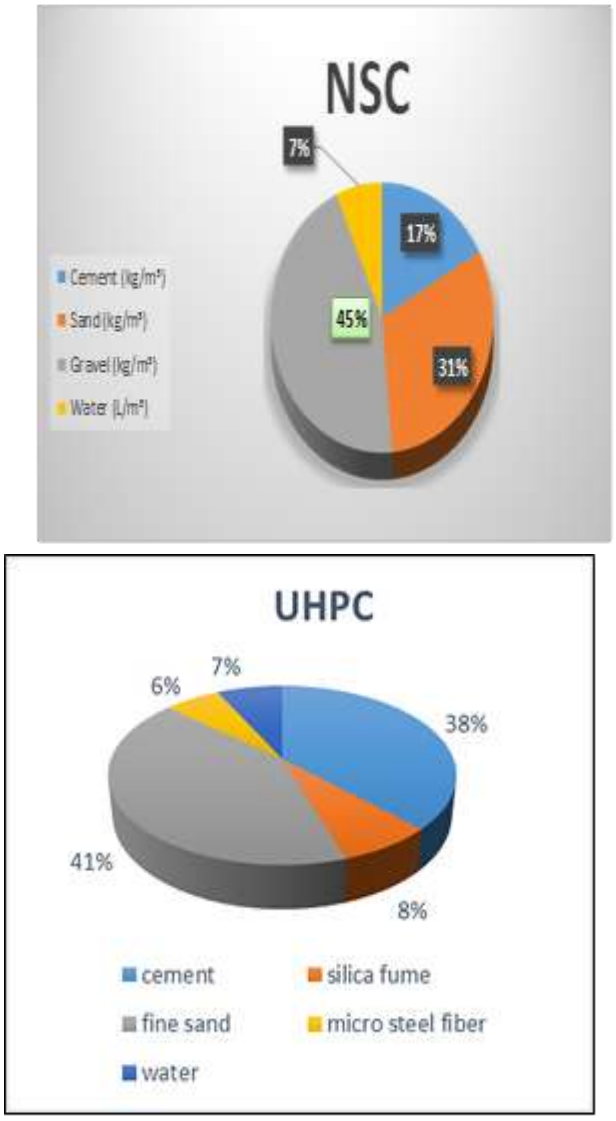

Fig.2: Material proportions in NSC and UHPC mixture

The external strengthening system consisted of a single layer of SikaWrap®-230 C/45 CFRP sheet bonded to the tension face of the beams using Sikadur®-330 two-component epoxy adhesive. The CFRP sheet was cut to the required strengthening dimensions of 150 mm × 450 mm, with the fibers oriented parallel to the longitudinal axis of the beam. According to the manufacturer's data, the CFRP sheet had a tensile strength of 4300 MPa,

an elastic modulus of 238 GPa, an elongation at break of 1.8%, and an equivalent thickness of 1.0 mm when applied with Sikadur®-330. The epoxy adhesive was mixed at a component A-to-component B ratio of 4:1 by mass and allowed to cure for seven days before long-term exposure.

Fig.3: Sikadur®-330 epoxy adhesive used for bonding CFRP sheets to the concrete

All beam specimens were reinforced with deformed steel bars. The longitudinal reinforcement consisted of two 12 mm bars in the tension zone and two 6 mm bars in the compression zone, while 6 mm closed stirrups were provided at 80 mm spacing along the beam span. For the long-term durability condition considered in this paper, the strengthened specimens were exposed to a 3.5% magnesium sulfate ($MgSO_4$) solution for 120 days after CFRP bonding and epoxy curing. This exposure regime was adopted to evaluate the ability of different surface preparation techniques to maintain CFRP–epoxy–concrete interface performance under sulfate conditioning.

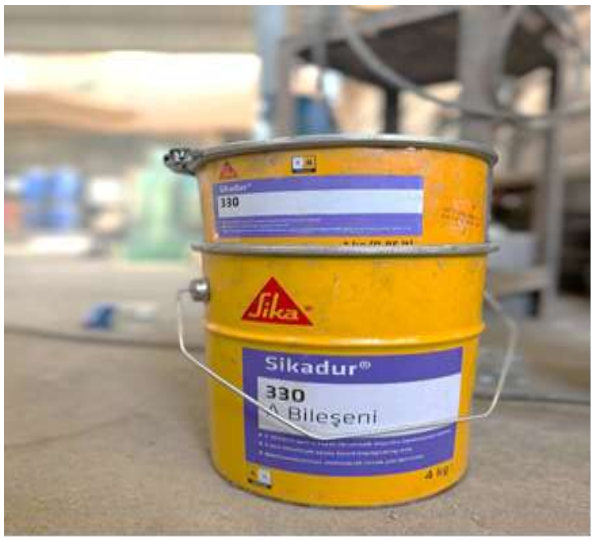

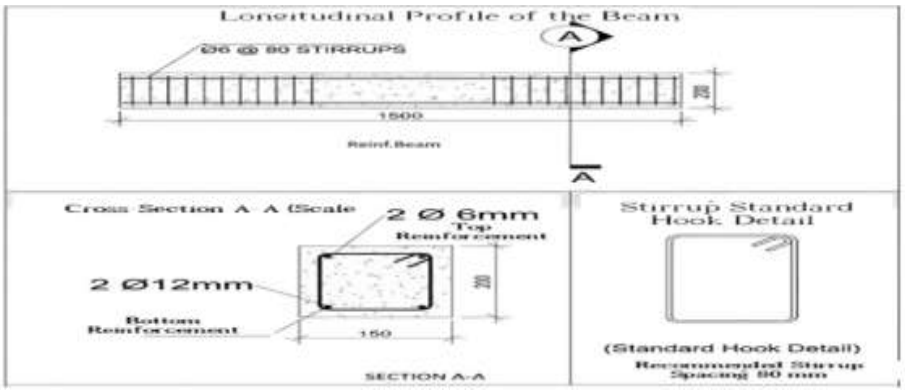

Fig.4: Geometrical details and reinforcement layout of the tested beam

Specimen Matrix

The experimental matrix considered in this paper was limited to the long-term exposure group. This group consisted of twelve reinforced concrete beam specimens, including six normal-strength concrete (NSC) beams and six ultra-high-performance concrete (UHPC) beams. For each concrete type, one unstrengthened control beam was used as a reference specimen, while the remaining five beams were strengthened with a single externally bonded CFRP layer after applying different surface preparation techniques. These techniques included mechanical grinding, vertical grooves, 45° inclined grooves, sandblasting, and diluted HCl treatment. After CFRP bonding and seven days of epoxy curing, all strengthened specimens were fully immersed in a 3.5% $MgSO_4$ solution for 120 days before flexural testing. The specimen designation, concrete type, surface preparation technique, strengthening condition, and exposure regime are summarized in Table 1.

Table 1. Experimental Matrix of long-term $MgSO_4$-conditioned beam specimens

Specimen ID	Concrete Type	Surface Preparation Technique	Exposure Type
LNC	Normal Concrete	Control specimen / without CFRP strengthening	Long-term
LNG	Normal Concrete	Mechanical grinding	Long-term
LNV	Normal Concrete	Vertical grooves	Long-term
LNI	Normal Concrete	45° inclined grooves	Long-term
LNH	Normal Concrete	Diluted HCl treatment	Long-term
LNS	Normal Concrete	Sandblasting	Long-term
LUC	Ultra-High-Performance Concrete (UHPC)	Control specimen / without CFRP strengthening	Long-term
LUG	Ultra-High-Performance Concrete (UHPC)	Mechanical grinding	Long-term
LUV	Ultra-High-Performance Concrete (UHPC)	Vertical grooves	Long-term
LUI	Ultra-High-Performance Concrete (UHPC)	45° inclined grooves	Long-term
LUH	Ultra-High-Performance Concrete (UHPC)	Diluted HCl treatment	Long-term

LUS	Ultra-High-Performance Concrete (UHPC)	Sandblasting	Long-term

Surface Preparation Techniques

Five surface preparation techniques were adopted before bonding the CFRP sheet to the tension face of the strengthened beams. The preparation zone was located within the middle third of the beam span, corresponding to the CFRP bonding region. The purpose of these techniques was to modify the concrete surface texture, improve epoxy adhesion, enhance mechanical interlock, and reduce the possibility of premature debonding after long-term $MgSO_4$ exposure.

3. Results and Discussion

Mechanical Grinding

Mechanical grinding was used to remove the weak superficial cement paste layer and produce a relatively uniform roughened surface. The grinding process was applied within the CFRP bonding zone in both longitudinal and transverse directions to improve the contact between the epoxy adhesive and the concrete substrate. After grinding, the treated surface was cleaned to remove dust, loose particles, and remaining laitance, then left to dry completely before applying the epoxy adhesive and bonding the CFRP sheet.

Vertical Grooving

The vertical grooving technique was adopted to increase the effective bonded area and enhance mechanical interlock at the CFRP–epoxy–concrete interface. Parallel grooves were formed perpendicular to the longitudinal axis of the beam within the CFRP bonding region. The grooves had an average spacing of approximately 43 mm, a depth of about 4 mm, and a width of about 3.5 mm. This configuration allowed the epoxy adhesive to penetrate into the grooves and form mechanical shear keys, thereby improving resistance to interfacial slip and premature debonding.

Inclined Grooving at 45°

Inclined grooves were formed at an angle of 45° relative to the longitudinal axis of the beam to investigate the influence of groove orientation on stress transfer and debonding resistance. This preparation method was intended to modify the direction of interfacial shear transfer and create inclined mechanical keys within the bonded zone. The inclined groove system was also expected to interrupt the direct propagation of interfacial separation along the CFRP direction and improve the redistribution of shear and peel stresses along the bonded interface.

Sandblasting

Sandblasting was used to remove the weak surface layer and produce a rough, open-textured bonding surface. The process was applied uniformly over the CFRP bonding region until the superficial cement paste was removed and fine/coarse aggregate particles became exposed. This treatment increased the surface roughness and improved the potential for epoxy penetration and mechanical interlock. After sandblasting, the surface was carefully cleaned from residual sand, dust, and loose particles before epoxy application and CFRP bonding.

Chemical Etching with HCl

Chemical etching was carried out using diluted hydrochloric acid to partially dissolve the weak superficial cement paste layer and increase the micro-roughness of the concrete surface. A diluted HCl solution was applied uniformly over the CFRP bonding zone and allowed to react with the surface until the required surface interaction was achieved. After the reaction, the surface was thoroughly rinsed and brushed to remove acid residues and reaction products, then left to dry completely before applying the epoxy adhesive. This cleaning step was essential to avoid weakening the bond due to residual acid or moisture.

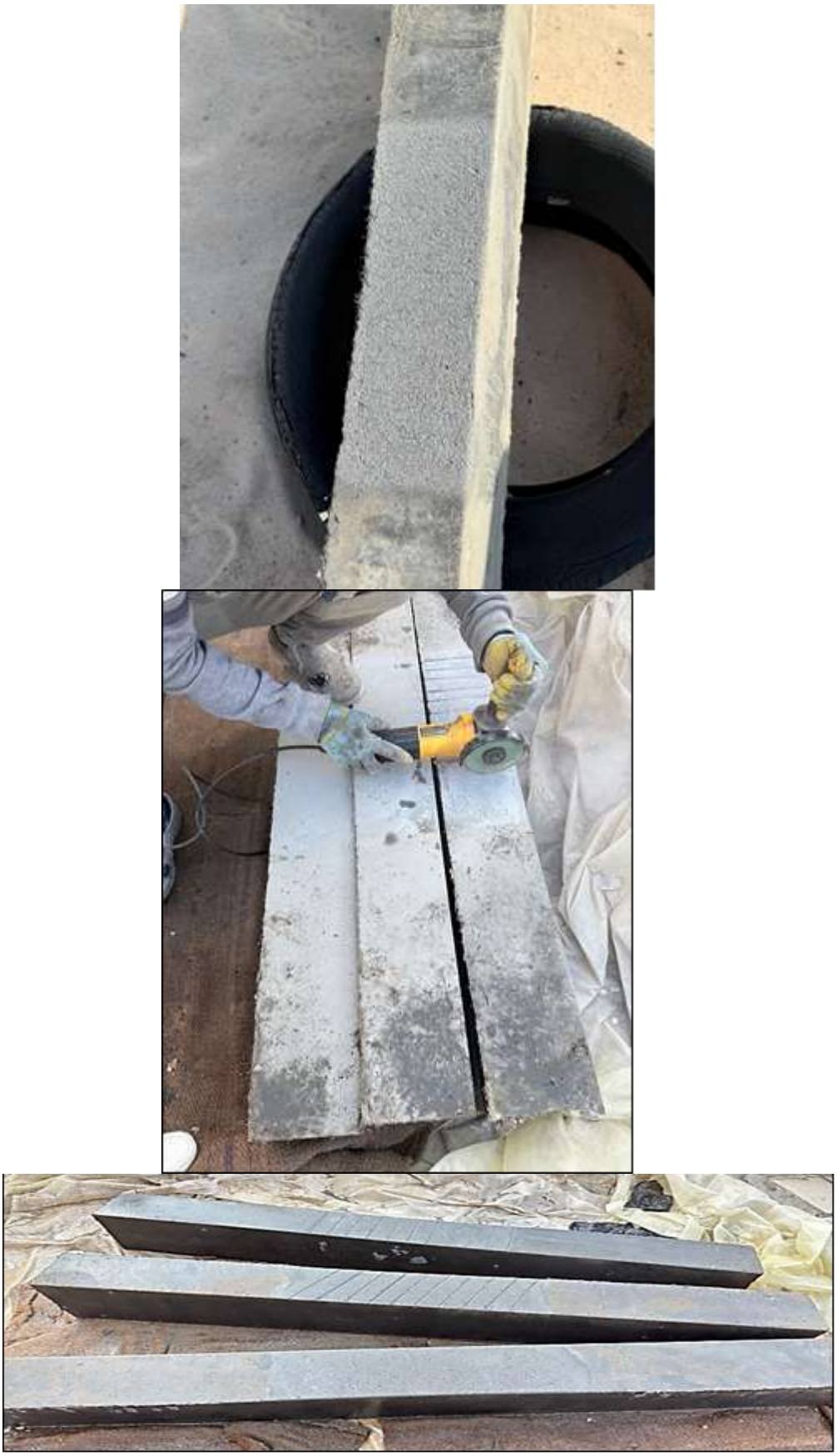

Fig 5: Surface preparation techniques used before CFRP bonding.

CFRP Bonding Procedure

After completing the surface preparation process, the treated bonding region was cleaned and allowed to dry completely before applying the epoxy adhesive. A single layer

of CFRP sheet was bonded to the tension face of each strengthened beam within the prepared middle-span region. Sikadur®-330 two-component epoxy adhesive was used to bond the CFRP sheet to the concrete substrate. The adhesive components were mixed according to the manufacturer's recommended ratio and applied uniformly over the prepared surface to ensure continuous contact between the CFRP sheet, epoxy layer, and concrete substrate. The CFRP fibers were oriented parallel to the longitudinal axis of the beam to enhance flexural resistance. After installation, the strengthened specimens were left to cure for seven days before being subjected to long-term $MgSO_4$ conditioning.

Fig.6: specimen preparation prior to CFRP bonding.

Long-Term $MgSO_4$ Conditioning

The long-term exposure regime was adopted to evaluate the durability-related performance of the CFRP–epoxy–concrete interface under aggressive sulfate conditions. After surface preparation, CFRP bonding, and seven days of epoxy curing, the long-term strengthened specimens were fully immersed in a magnesium sulfate ($MgSO_4$) solution. The exposure medium was prepared at a concentration of 3.5% $MgSO_4$ by mass to represent a sulfate-rich environment. The specimens were kept continuously immersed in the solution for 120 days before flexural testing.

During the conditioning period, the solution level was regularly monitored to ensure complete immersion of the strengthened specimens. When the water level decreased due to evaporation, water and $MgSO_4$ salts were added according to the required concentration to maintain relatively stable exposure conditions. This procedure was adopted to assess the ability of each surface preparation technique to preserve bond stability, strengthening efficiency, and failure-mode resistance after prolonged sulfate exposure**.**

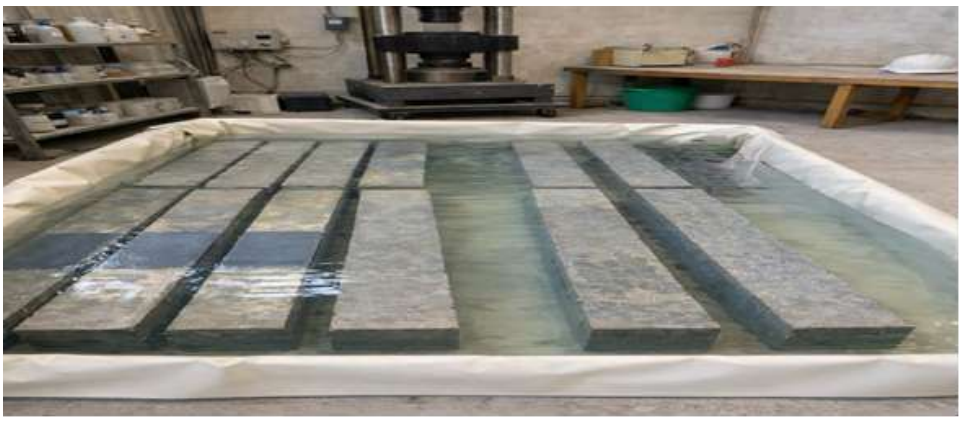

Fig.7: Long-term immersion of strengthened beam specimens in $MgSO_4$ solution.

Flexural Test Setup and Recorded Parameters

All beam specimens were tested under simply supported boundary conditions using a two-point loading system. The clear span was 1300 mm, while the distance between the two loading points was 430 mm, producing a constant-moment region at mid-span. The load was applied through a steel spreader girder to ensure equal load distribution at the two loading points. Steel bearing plates and rollers were used at the supports and loading locations to minimize local stress concentration and prevent premature local crushing.

Before testing, the beam surfaces were painted with white emulsion and marked with reference lines to facilitate crack observation and documentation. Vertical deflection was measured using laser-based LVDTs connected to an independent reference frame, while the applied load was recorded using the testing machine load cell. The beams were loaded monotonically until failure, and the test data were continuously recorded through a computerized data acquisition system.

The main recorded parameters included the load–deflection response, first-cracking load, ultimate load, mid-span deflection, crack initiation and propagation, and final failure mode. These measurements were used to evaluate the long-term flexural performance, stiffness response, ductility-related behavior, energy absorption, and debonding characteristics of the $MgSO_4$-conditioned CFRP-strengthened beams.

Ultimate Load and Strengthening Efficiency

The ultimate load results clearly indicate that CFRP strengthening remained effective after 120 days of $MgSO_4$ exposure; however, the level of improvement depended strongly on the adopted surface preparation technique and concrete substrate type. For the NSC group, the unstrengthened control beam LNC reached an ultimate load of 120.87 kN. The strengthened beams LNG, LNV, LNI, LNS, and LNH achieved ultimate loads of 122.55, 133.24, 132.58, 145.70, and 129.22 kN, respectively. Accordingly, sandblasting produced the highest ultimate load among the $MgSO_4$-conditioned NSC beams, corresponding to a strengthening efficiency of 20.55% relative to LNC. Vertical grooving and 45° inclined grooving also improved the ultimate capacity, with increases of 10.24% and 9.69%, respectively, while HCl treatment and mechanical grinding produced more limited improvements. For the UHPC group, the unstrengthened control beam LUC reached an ultimate load of 160.17 kN. The strengthened beams LUG, LUV, LUI, LUH, and LUS achieved ultimate loads of 170.47, 187.66, 202.89, 175.38, and 205.20 kN, respectively. Similar to the NSC group, sandblasting provided the highest ultimate load after $MgSO_4$ exposure, with an increase of 28.12% compared with LUC. The 45° inclined grooving technique achieved a very close response, increasing the ultimate load by 26.67%, which indicates a highly efficient and stable bond condition. Overall, the UHPC beams exhibited higher load-carrying capacity than their corresponding NSC specimens, confirming that UHPC provided a stronger and more stable substrate for CFRP strengthening under long-term sulfate exposure.

Table 2. Ultimate load and strengthening efficiency of long-term $MgSO_4$-conditioned beams

Specimen	Concrete type	Surface preparation	Ultimate load, Pu (kN)	Increase relative to control (%)
LNC	NSC	Control	120.87	—
LNG	NSC	Mechanical grinding	122.55	1.39
LNV	NSC	Vertical grooves	133.24	10.24
LNI	NSC	45° inclined grooves	132.58	9.69
LNS	NSC	Sandblasting	145.70	20.55
LNH	NSC	HCl treatment	129.22	6.91
LUC	UHPC	Control	160.17	—

LUG	UHPC	Mechanical grinding	170.47	6.43
LUV	UHPC	Vertical grooves	187.66	17.16
LUI	UHPC	45° inclined grooves	202.89	26.67
LUH	UHPC	HCl treatment	175.38	9.50
LUS	UHPC	Sandblasting	205.20	28.12

Load–Deflection Response

The load–deflection curves of the long-term $MgSO_4$-conditioned beams provide a clear indication of the influence of surface preparation technique on the flexural response and bond stability of the CFRP-strengthened system. In general, all specimens exhibited an initial approximately linear response before first cracking, followed by nonlinear behavior associated with crack development, stiffness degradation, reinforcement yielding, and progressive damage accumulation. The strengthened beams generally sustained higher loads than their corresponding unstrengthened control specimens, confirming that the CFRP system remained effective after 120 days of sulfate exposure. However, the degree of improvement and the shape of the post-cracking response varied depending on the surface preparation method and concrete substrate type.

For the NSC group, the control specimen LNC showed the lowest load-carrying capacity, while the CFRP-strengthened beams exhibited improved post-cracking resistance. Among the strengthened NSC specimens, LNS showed the most favorable strength response, indicating that sandblasting provided a more effective roughened surface for epoxy bonding and stress transfer after sulfate conditioning. The grooved specimens, particularly LNV and LNI, also improved the response compared with the control beam, reflecting the contribution of mechanical interlock to load transfer across the CFRP–epoxy–concrete interface. However, the very large deformation observed in some specimens should be interpreted carefully, since increased deflection may reflect progressive stiffness degradation rather than superior bond efficiency alone.

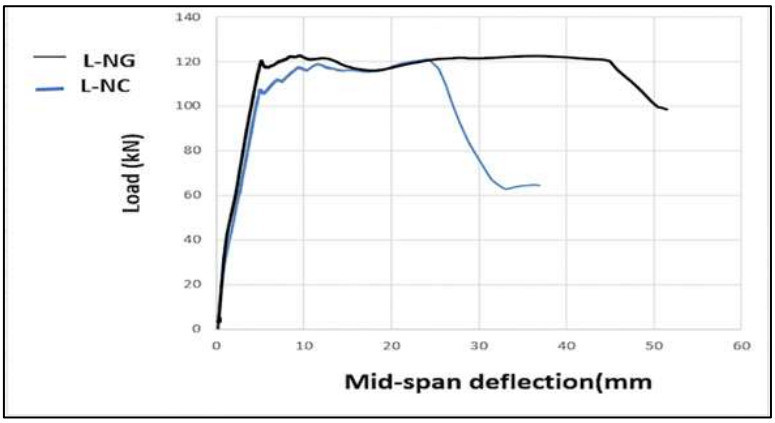

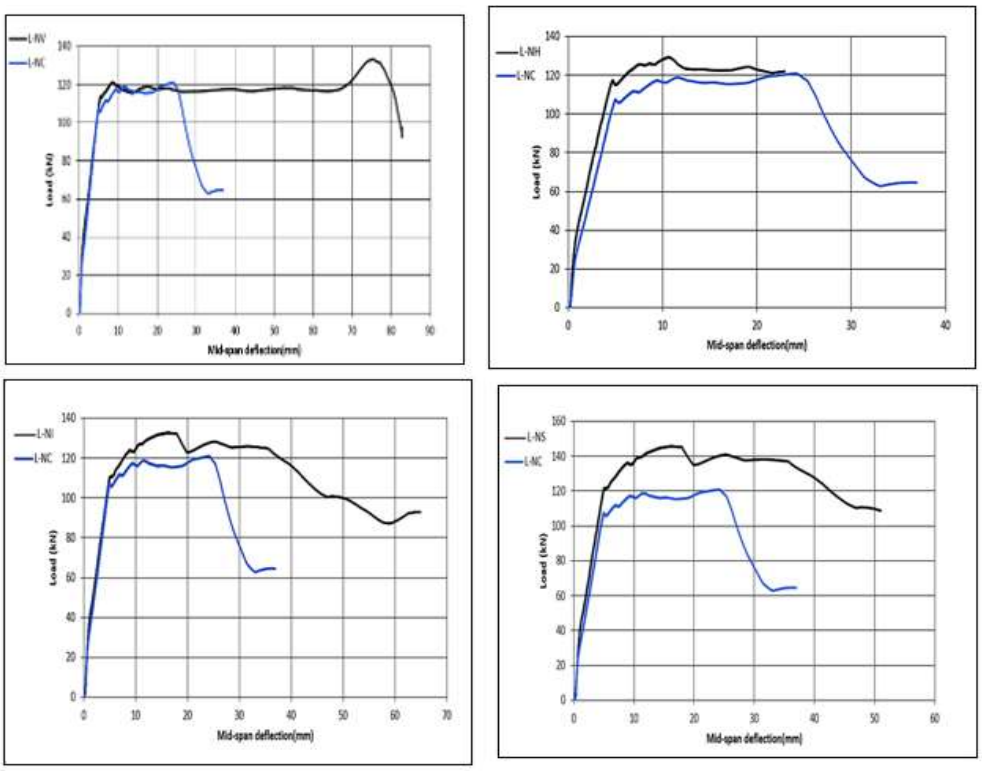

Fig8. Load–deflection curves of long-term $MgSO_4$-conditioned NSC beams

For the UHPC group, the load–deflection curves showed higher load resistance and a more stable structural response than those of the corresponding NSC beams. This behavior can be attributed to the higher compressive and tensile capacity of UHPC, its improved crack-control ability, and the contribution of steel fibers in limiting crack widening. The LUS specimen achieved the highest ultimate load, confirming the effectiveness of sandblasting in producing a strong and uniform bonding surface. The LUI specimen showed a very close performance, indicating that 45° inclined grooves provided an efficient bond condition by improving mechanical interlock and redistributing interfacial stresses. Overall, the load–deflection response demonstrates that surface preparation controlled not only the peak load, but also the post-cracking stiffness, deformation development, and stability of the CFRP–epoxy–concrete interface after long-term $MgSO_4$ exposure.

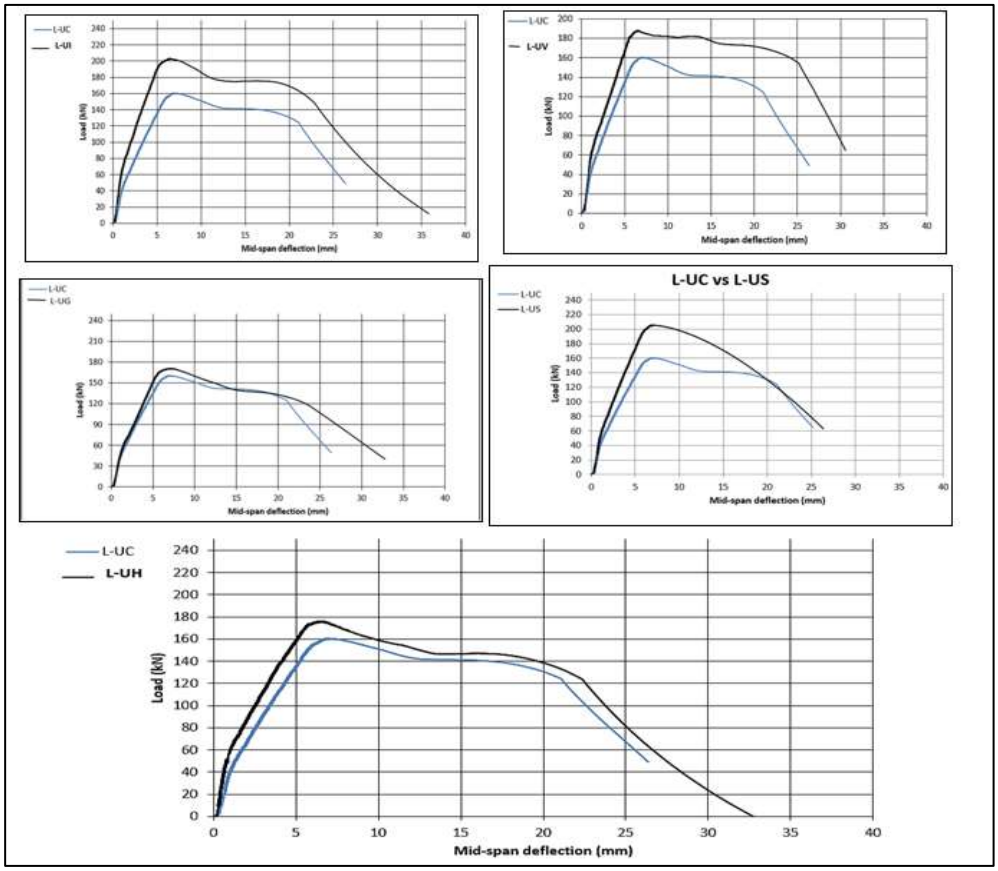

Fig 9. Load–deflection curves of long-term $MgSO_4$-conditioned UHPC beams.

Stiffness Response

The stiffness response was evaluated to provide a more direct indication of the effectiveness of stress transfer across the CFRP–epoxy–concrete interface after long-term $MgSO_4$ exposure. In this study, the secant stiffness was considered a useful parameter because it reflects the ability of the strengthened beam to resist deflection at a defined load level, rather than relying only on the ultimate load capacity. Therefore, stiffness was used as a complementary indicator for assessing the influence of surface preparation technique on bond stability and composite action.

For the $MgSO_4$-conditioned NSC beams, the stiffness response was strongly affected by the adopted surface preparation technique. Although CFRP strengthening generally improved the ultimate load, the stiffness response was not governed by strength increase alone. Some specimens showed larger deformation and progressive stiffness degradation after cracking, indicating that higher load capacity does not necessarily mean superior bond efficiency. This behavior confirms that the long-term response of CFRP-strengthened NSC beams should be interpreted by combining stiffness with the complete load–deflection curve, crack development, and failure mode.

For the $MgSO_4$-conditioned UHPC beams, all CFRP-strengthened specimens exhibited higher secant stiffness than the unstrengthened control specimen. The control beam LUC recorded a stiffness of 27.81 kN/mm, whereas LUG, LUV, LUI, LUH, and LUS recorded stiffness values of 30.82, 35.04, 40.96, 34.97, and 35.63 kN/mm, respectively. The highest stiffness was achieved by LUI, corresponding to an increase of 47.28% relative to LUC. This indicates that 45° inclined grooving provided the most effective stiffness-related response in the UHPC group after $MgSO_4$ conditioning. The improved performance can be attributed to the ability of inclined grooves to enhance mechanical interlock, modify the direction of interfacial stress transfer, and improve the redistribution of shear and peel stresses along the bonded interface.

Overall, the stiffness results demonstrate that surface preparation controlled not only the ultimate strength but also the deformation resistance and interface stability of the CFRP-strengthened beams. Sandblasting produced the highest ultimate load, while 45°

inclined grooving provided the most favorable stiffness response in UHPC after long-term sulfate exposure. This distinction is important because it shows that the best surface preparation technique may depend on the selected performance criterion.

Table 3. Secant stiffness of long-term $MgSO_4$-conditioned NSC and UHPC beams

Beam ID	**0.75 Pu.** **(KN)**	**Deflection at 0.75 Pu. (mm)**	**Stiffness, K (KN/mm)**	**Difference from reference beam %**
LNC	90.65	18.12	5.00	-----
LNG	91.91	7.16	12.83	156.6%
LNV	99.75	56.52	1.76	64.8%
LNI	99	11.84	8.36	67.2%
LNH	96.75	8	12.09	141.85%
LNS	109.27	12.04	9.07	81.4%
LUC	120.13	4.32	27.81	0.00
LUG	127.85	4.15	30.82	+10.82
LUV	140.75	4.02	35.04	+25.99
LUI	152.17	3.72	40.96	+47.28
LUH	131.76	3.77	34.97	+25.75
LUS	153.90	4.32	35.63	+28.12

Ductility and Deformation Capacity

Ductility was evaluated using the displacement ductility index, defined as the ratio between the deflection corresponding to the ultimate load and the notional yield deflection obtained from the idealized bilinear load–deflection response. This parameter was used to assess the deformation capacity of the long-term $MgSO_4$-conditioned beams and to clarify whether the strengthened system could sustain additional deformation before reaching the maximum load.

For the NSC group, the control beam LNC recorded a ductility index of 7.86. The CFRP-strengthened specimens LNG, LNV, LNI, LNH, and LNS recorded ductility values of 3.53, 22.69, 5.08, 4.15, and 5.00, respectively. The exceptionally high ductility value of LNV was mainly associated with its very large ultimate deflection rather than with superior bond efficiency alone. Therefore, this value should be interpreted as an indication of a highly deformable response accompanied by substantial stiffness degradation. In contrast, LNI and LNS showed more balanced ductility values, indicating that inclined grooving and sandblasting allowed the strengthened NSC beams to maintain reasonable deformation capacity while improving load resistance after sulfate exposure.

For the UHPC group, the control beam LUC recorded a ductility index of 3.63, while LUG, LUV, LUI, LUH, and LUS recorded ductility values of 4.49, 4.16, 4.42, 4.84, and 3.65, respectively. Compared with the NSC beams, the UHPC specimens exhibited a narrower range of ductility variation, indicating a more stable deformation response after $MgSO_4$ conditioning. The highest ductility in the UHPC group was obtained by LUH, followed by LUG and LUI. However, the ductility of LUS remained close to the control beam, despite achieving the highest ultimate load, suggesting that sandblasting enhanced strength without producing excessive deformation. Meanwhile, LUI combined high load capacity, high stiffness, and adequate ductility, reflecting a balanced long-term structural response.

Table 4. Ductility indices of long-term $MgSO_4$-conditioned NSC and UHPC beams

Specimen ID	Pu (KN)	δu (mm)	δy (mm)	μ = δu / δy
L-NC	120.87	24.17	3.08	7.86
L-NG	122.55	9.55	2.71	3.53
L-NV	133	75.37	3.32	22.69
L-NI	132	15.79	3.11	5.08
L-NH	129	10.67	2.57	4.15
L-NS	145.7	16.06	3.21	5.00
L-UC	160.17	7.02	1.932	3.632
L-UG	170.47	7.04	1.569	4.490
L-UV	187.66	6.51	1.564	4.158
L-UI	202.89	6.43	1.455	4.421
L-UH	175.68	6.27	1.352	4.835
L-US	205.20	7.02	1.921	3.653

Overall, the ductility results show that deformation capacity was strongly affected by both substrate type and surface preparation technique. A high ductility index alone should not be considered sufficient evidence of superior strengthening performance, particularly when it results from excessive deflection and stiffness degradation. Therefore, ductility must be interpreted together with ultimate load, stiffness, energy absorption, and failure mode to provide a reliable assessment of the long-term performance of CFRP-strengthened beams exposed to $MgSO_4$ solution.

Energy Absorption

Energy absorption was evaluated from the area under the load–deflection curve and was used as a complementary indicator of the ability of the beam to sustain load and deformation during loading. In the present study, two energy-related parameters were considered: the energy absorbed up to the peak load, (E_u), and the total absorbed energy up to the end of the test, (E_{end}). This parameter is important for assessing the long-term performance of CFRP-strengthened beams because it reflects not only the peak load capacity, but also the post-cracking and post-peak deformation response.

For the $MgSO_4$-conditioned NSC group, the control specimen LNC recorded a total absorbed energy of 3555.14 kN·mm. The strengthened specimens LNG, LNV, LNI, LNH, and LNS recorded (E_{end}) values of 5766.76, 9519.45, 7498.45, 8477.60, and 6420.64 kN·mm, respectively. The highest total absorbed energy was obtained by LNV; however, this result should be interpreted carefully because it was mainly associated with the very

large deformation developed before failure. Therefore, the high energy absorption of LNV does not necessarily indicate the most efficient bond condition, but rather reflects a highly deformable response accompanied by considerable stiffness degradation. In contrast, LNI, LNH, and LNS showed improved energy absorption together with more controlled deformation behavior, indicating a more balanced long-term response.

For the $MgSO_4$-conditioned UHPC group, the control specimen LUC recorded a total absorbed energy of 3141.73 kN·mm, while LUG, LUV, LUI, LUH, and LUS recorded values of 3852.53, 4611.10, 4684.12, 3656.84, and 3783.83 kN·mm, respectively. All CFRP-strengthened UHPC specimens absorbed more energy than the control beam, confirming that the CFRP strengthening system remained active after 120 days of sulfate exposure. The highest total absorbed energy was recorded by LUI, followed closely by LUV, which indicates that inclined and vertical grooves were effective in preserving composite action and allowing the beams to sustain load over a wider deformation range. Although LUS achieved the highest ultimate load, its total absorbed energy was lower than that of LUI and LUV, confirming that peak strength and energy absorption do not necessarily follow the same trend.

Overall, the energy absorption results confirm that surface preparation significantly influenced the long-term structural response of CFRP-strengthened beams. However, energy absorption should not be used alone to judge bond efficiency, since high energy values may result from excessive deformation rather than superior interface performance. Therefore, the energy results must be interpreted together with ultimate load, stiffness, ductility, load–deflection behavior, and failure mode to identify the most reliable surface preparation technique under $MgSO_4$ exposure.

Table 5. Energy absorption values of long-term $MgSO_4$-conditioned NSC and UHPC beams

Specimen ID	Eu (KN·mm)	E end (KN·mm)
L-NC	2517.47	3555.14
L-NG	866.99	5766.76
L-NV	8619.09	9519.45
L-NI	1706.95	7498.45
L-NH	1057.19	8477.60
L-NS	1875.08	6420.64
L-UC	680.97	3141.73
L-UG	742.05	3852.53
L-UV	747.02	4611.10
L-UI	829.47	4684.12
L-UH	734.41	3656.84
L-US	872.44	3783.83

Overall Discussion of Long-Term Performance

The overall results demonstrate that the long-term performance of CFRP-strengthened beams exposed to $MgSO_4$ solution was strongly governed by the combined effect of concrete substrate type and surface preparation technique. Although all strengthened specimens were subjected to the same exposure regime, their structural responses differed clearly in terms of ultimate load, stiffness, ductility, and energy absorption. This confirms that surface preparation was not merely a construction procedure, but a controlling factor affecting the durability and efficiency of the CFRP–epoxy–concrete interface.

For the NSC group, sandblasting produced the highest ultimate load, indicating that removing the weak surface layer and producing an open roughened texture improved the ability of the epoxy adhesive to develop effective mechanical interlock with the concrete

substrate. Vertical and inclined grooves also improved the structural response by increasing the effective bonded area and providing mechanical shear keys within the interface. However, the response of some NSC specimens showed larger deformation and stiffness degradation, indicating that the performance of CFRP strengthening after sulfate exposure cannot be evaluated by strength increase alone.

For the UHPC group, the strengthened beams exhibited higher load resistance and more stable response than the corresponding NSC specimens. This behavior can be attributed to the superior mechanical properties of UHPC, its improved crack-control capacity, and the contribution of steel fibers in limiting crack widening. Among the UHPC specimens, sandblasting achieved the highest ultimate load, while 45° inclined grooving provided the most favorable stiffness-related response and a balanced combination of strength, stiffness, and deformation capacity. This indicates that mechanical roughening and groove-based preparation techniques were particularly effective for maintaining bond stability in the dense UHPC substrate after $MgSO_4$ conditioning.

Overall, sandblasting can be considered the most effective technique when the main performance criterion is ultimate load enhancement, whereas 45° inclined grooving provides a more balanced long-term response in terms of stiffness, bond stability, and deformation behavior, especially for UHPC beams. Chemical etching showed a comparatively less consistent response, suggesting that purely chemical surface modification may be more sensitive to long-term sulfate conditioning. Therefore, mechanical surface preparation methods are recommended for improving the long-term reliability of CFRP-strengthened NSC and UHPC beams exposed to sulfate-rich environments.

4. Conclusion

Based on the experimental results of the long-term $MgSO_4$-conditioned CFRP-strengthened NSC and UHPC beams, the following conclusions can be drawn:

a. CFRP strengthening remained effective after 120 days of exposure to 3.5% $MgSO_4$ solution; however, the achieved strengthening efficiency was governed by both the concrete substrate type and the adopted surface preparation technique. This confirms that the durability of the CFRP-strengthened system cannot be evaluated by CFRP application alone, but must be related to the quality of the CFRP–epoxy–concrete interface.

b. For the NSC group, sandblasting produced the highest ultimate load, increasing the capacity from 120.87 kN for the control beam to 145.70 kN, corresponding to a 20.55% improvement. This improvement indicates that removing the weak superficial layer and producing an open roughened surface enhanced epoxy adhesion and mechanical interlock after sulfate conditioning.

c. For the UHPC group, sandblasting also achieved the highest ultimate load, increasing the capacity from 160.17 kN for the control beam to 205.20 kN, corresponding to a 28.12% improvement. This confirms that sandblasting was effective in activating the CFRP contribution even when applied to the dense and low-permeability UHPC substrate.

d. The 45° inclined grooving technique provided the most favorable stiffness-related response in the UHPC group. The LUI specimen achieved a secant stiffness of 40.96 kN/mm, representing a 47.28% increase relative to the UHPC control beam. This behavior suggests that inclined grooves improved mechanical interlock and promoted a more efficient redistribution of interfacial shear and peel stresses along the CFRP–epoxy–UHPC interface.

e. Ductility and energy absorption results showed that high deformation capacity should not be interpreted alone as evidence of superior bond performance. In particular, the very high ductility and energy absorption observed in the NSC vertical-grooved specimen were mainly associated with excessive deflection and stiffness degradation. Therefore, ductility and energy absorption must be evaluated together with ultimate load, stiffness, and load–deflection behavior.

f. The UHPC specimens exhibited a more stable and consistent long-term response than the corresponding NSC specimens. This behavior is attributed to the higher mechanical properties of UHPC, the contribution of steel fibers in crack control, and the ability of properly prepared UHPC surfaces to maintain composite action after $MgSO_4$ exposure.
g. Overall, sandblasting can be considered the most effective surface preparation technique when the target is maximum load enhancement, whereas 45° inclined grooving provides a more balanced long-term response in terms of strength, stiffness, deformation behavior, and interface reliability. Chemical etching showed a less consistent response and should be used cautiously in sulfate-conditioned CFRP-strengthened systems.
h. The results confirm that surface preparation should be treated as a durability-design variable rather than a routine construction step in CFRP-strengthened concrete members exposed to sulfate-rich environments

REFERENCES

[1] J.-G. Teng, J.-F. Chen, S. T. Smith, and L. Lam, FRP-Strengthened RC Structures. Chichester, UK: John Wiley & Sons, 2002.
[2] J. G. Teng, J. F. Chen, and S. T. Smith, "Debonding failures in FRP-strengthened RC beams: Failure modes, existing research and future challenges," in Composites in Construction: A Reality, 2001, pp. 139–148.
[3] O. Buyukozturk, O. Gunes, and E. Karaca, "Progress on understanding debonding problems in reinforced concrete and steel members strengthened using FRP composites," Construction and Building Materials, vol. 18, no. 1, pp. 9–19, 2004.
[4] M. Alkaysi, S. El-Tawil, Z. Liu, and W. Hansen, "Effects of silica powder and cement type on durability of ultra- high -performance concrete (UHPC)," Cement and Concrete Composites, vol. 66, pp. 47–56, 2016.
[5] Y. Yin and Y. Fan, "Influence of roughness on shear bonding performance of CFRP–concrete interface," Materials, vol. 11, no. 10, p. 1875, 2018.
[6] R. Z. Al-Rousan and M. F. AL-Tahat, "Consequence of surface preparation techniques on the bond behavior between concrete and CFRP composites," Construction and Building Materials, vol. 212, pp. 362–374, 2019.
[7] S. Soares, J. Sena-Cruz, J. R. Cruz, and P. Fernandes, "Influence of surface preparation method on the bond behavior of externally bonded CFRP reinforcements in concrete," Materials, vol. 12, no. 3, p. 414, 2019.
[8] J. Li, Z. Wu, C. Shi, Q. Yuan, and Z. Zhang, "Durability of ultra-high performance concrete – A review," Construction and Building Materials, vol. 255, p. 119296, 2020.
[9] H. Masrafat, "The effect of sulfate exposure on the mechanical properties of conventional Portland composite cement concrete," Journal of Civil Engineering, vol. 39, no. 2, pp. 92–100, 2024.
[10] G. Zhao, J. Li, and F. Han, "Sulfate-induced degradation of cast-in-situ concrete influenced by magnesium," Construction and Building Materials, vol. 199, pp. 194–206, 2019.
[11] F. Al-Mahmoud, J.-M. Mechling, and M. Shaban, "Bond strength of different strengthening systems—Concrete elements under freeze–thaw cycles and salt water immersion exposure," Construction and Building Materials, vol. 70, pp. 399–409, 2014.
[12] A. Uthaman, G. Xian, S. Thomas, Y. Wang, Q. Zheng, and X. Liu, "Durability of an epoxy resin and its carbon fiber-reinforced polymer composite upon immersion in water, acidic, and alkaline solutions," Polymers, vol. 12, no. 3, p. 614, 2020.
[13] F. Zhang, J.-G. Dai, Z. Wang, M. Wang, Y. Leng, and Q. Xu, "Bond durability of epoxy and cement-bonded CFRP reinforcement to concrete interfaces subject to water immersion," Materials and Structures, vol. 54, no. 2, Article 53, 2021.
[14] R. Cruz, L. Correia, A. Dushimimana, S. Cabral-Fonseca, and J. Sena-Cruz, "Durability of epoxy adhesives and carbon fibre reinforced polymer laminates used in strengthening systems: Accelerated ageing versus natural ageing," Materials, vol. 14, no. 6, p. 1533, 2021.
[15] P. Fernandes, J. Sena-Cruz, J. Xavier, P. Silva, E. Pereira, and J. R. Cruz, "Durability of bond in NSM CFRP-concrete systems under different environmental conditions," *Composites Part B: Engineering*, vol. 138, pp. 19–34, 2018.